# Hyperfluorescence™: Groundbreaking Materials Advancement for Diverse Color -Gamut Applications

***Shuo-Hsien Cheng, Masataka Yamashita, Motoki Toganoh, Hayato Kakizoe, Taro Hamasaki, Ayataka Endo, Hiroaki Ozawa***
**Kyulux, Inc., Fukuoka, Japan**

## Abstract
***Hyperfluorescence™ (HF), known as the most advanced OLED emitting technology, combines thermally activated delayed fluorescence (TADF) and fluorescence mechanisms enabling 100% internal quantum efficiency (IQE) and narrowband emission without using noble metals. By judicious materials selection, HF OLEDs can widely correspond to the application requirements of diverse color gamuts for the primary colors of green, red and blue. Among our RGB achievements in this report, it is noteworthy that green HF exhibited a narrow bottom-emission bandwidth of 28 nm, leading to an outstanding estimated TE efficiency of 199 cd/A, while a significant $LT_{95}$ of 1,500 h was achieved for AdobeRGB chromaticity. Also, a deep-blue HF OLED achieved an unprecedented blue index of 417 cd/A/$CIE_y$ at CIEy = 0.05 by using a sky-blue TADF sensitizer, offering an expedited path for device lifespan improvement.***

## Author Keywords
Hyperfluorescence™; HF OLEDs; TADF; OLED; Electroluminescence; Emitting technology; Kyulux.

## 1. Introduction
Hyperfluorescence™ (HF) has been considered a promising next-generation emitting technology for organic light-emitting diodes (OLEDs). With the rapid expansion of the OLED market across applications such as mobiles, tablets, TVs, in-vehicle displays, and AR/VR devices, there is a consistent demand for lower power consumption, higher color fidelity (e.g., BT.2020 color gamut), and more cost-effective device stack designs to deliver an optimal user experience. Compared to commercial fluorescence and phosphorescence OLEDs, HF OLEDs, incorporating thermally activated delayed fluorescence (TADF) sensitizers and terminal fluorescence (FL) emitters, feature intrinsically narrow emission and 100% exciton utilization efficiency for red, green, and blue colors without the use of noble metals [1]. This provides HF OLED displays with unparalleled visual sharpness without compromising performance.

Inherited from conventional fluorescence OLEDs, the narrow emission bandwidth is one of the distinguishing features of HF OLEDs. In contrast to charge-transfer (CT) emission observed in phosphorescence and TADF, fluorescence dopants of HF OLEDs emit light from their locally excited (LE) state or their multi-resonant excited state. [2] This drastically eliminates the full-width at half-maximum (FWHM) of their emission spectrum and greatly improves color purity. Moreover, the narrow FWHM nature also minimizes energy loss when extracting light from microcavity or color filters, rendering a wider color gamut while simultaneously maintaining highly efficient properties under the same external quantum efficiency (EQE). Yet, compared to conventional fluorescence OLEDs, HF OLEDs can theoretically boost efficiency by up to four times owing to the incorporation of TADF sensitizers in addition to hosts and FL emitters. Unlike typical organic molecules, TADF overcomes quantum restrictions in light of its small singlet-triplet energy gap ($\Delta E_{ST}$), effectively harvesting both singlet and triplet excitons. Through the rapid reverse intersystem crossing (rISC), TADFs efficiently upconvert triplet energy to singlet energy, subsequently sensitizing terminal FL emitters and achieving a quantum efficiency approaching a unity. This capability offers OLED displays a promising path to markedly improve blue efficiency, as the current commercial blue OLEDs predominantly utilize triplet fusion FL emitters for their relatively stable device lifetimes [3].

Nevertheless, modern displays accommodate various color specifications depending on their specific application requirements. Among these, color fidelity is closely related to color gamut, which is defined by the area enclosed by the primary green, red, and blue colors in Commission internationale de l'éclairage (CIE) 1931 (x,y) coordinates. The larger the coverage within the CIE coordinates, the better the display can reproduce natural colors. Common color gamuts such as sRGB, DCI-P3, and AdobeRGB have appeared in everyday displays. Furthermore, BT.2020, released by the International Telecommunication Union (ITU) in 2012 [4], has become the latest wide color gamut (WCG) standard for the ultra-high definition (UHD) market. To accommodate these multiple color spaces, it is essential to develop pixels that can precisely describe the designated color points.

In this work, we report our latest progress in green, red, and blue HFs OLEDs development for diverse color gamuts. Regarding green performance, by incorporating our novel green TADFs and dopants, **G-HF1** and **G-HF2** achieved a bottom-emission EQE, FWHM, and $LT_{95}$ of 25.2%, 28 nm, and 1,500 h and 23.0%, 31 nm, and 970 h, respectively, at 10 mA/cm$^2$. Aiming for Adobe RGB and BT.2020 chromaticity, the top-emission efficiency of **G-HF1** and **G-HF2** was calculated to be 199 cd/A and 160 cd/A at $CIE_{x,y}$ = (0.210, 0.756) and (0.170, 0.776), respectively. We believe the remarkable performance, particularly in Adobe RGB chromaticity, meets industry application needs and will facilitate a smooth path to commercialization. In addition to green advances, our red HFs exhibiting robust performance with high color purity for both DCI-P3 and BT.2020 chromaticities are also on the way toward commercialization. Furthermore, we present our latest progress in blue HF development. An impressive blue index (BI) of 417 cd/A/$CIE_y$ was achieved by incorporating Kyulux's novel sky-blue TADF sensitizer into deep-blue HF, substantially exceeding that of blue fluorescence at around 250 cd/A/$CIE_y$. Through effective Föster resonance energy transfer (FRET) between the TADF sensitizer and terminal FL emitter, the FWHM of the bottom-emission HF was narrowed to 20 nm. This new approach opens a substantial path to realizing stable deep-blue HF OLEDs with delicately designed sky-blue TADF sensitizers. We believe that this major breakthrough will accelerate the development and commercialization of deep-blue HFs to meet display market demands.


*ISSN 0097-996X/25/5601-0648-$1.00 © 2025*

## 2. Experiments and Results

### *2.1. General*

With a judicious FL emitter selection, HF OLEDs can fulfill various color requirements, including green, red, blue, and even yellow. Through subtle structural modifications, the emission wavelength of the fluorescence dopants can be finely tuned to meet diverse application needs. For example, we have developed a series of dopants for green HFs to fulfill the color standards of DCI-P3, AdobeRGB, and BT.2020, as shown in Figure 1.

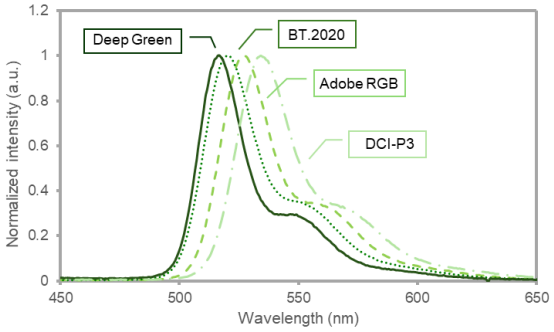


**Figure 1.** The PL spectrum of green Hyperfluorescence™ dopants for various color gamuts.

To examine the device performance, bottom emission (BE) devices were fabricated using the following configuration: anode/hole injection layer (HIL)/hole transporting layer (HTL)/electron blocking layer (EBL)/emitting layer (EML)/hole blocking layer (HBL)/electron transporting layer (ETL)/electron injection layer (EIL)/cathode, where indium-tin oxide (ITO), Liq, and Al were used as anode, EIL, and cathode, respectively.

Also, we simulate TE performance using Setfos 5.1 and employed a common device structure as follows: anode/HIL/HTL/EBL/EML/HBL/ETL/EIL/cathode, where ITO/Ag/ITO, LiF, and Mg:Ag (1:9), were used as anode, EIL, and cathode, respectively. The optical constants of each layer were measured by ellipsometry. The electroluminescence (EL) spectrum from the corresponding BE devices was used for simulation. We assumed all TE devices exhibit the same EQE as their respective BE devices. The recombination distribution was modeled as a delta function. The recombination position was 6 nm from the EBL (or 6 nm from the HBL for the green devices). Using the settings above, the HTL thickness was varied to optimize the microcavity length and monitor the maximum current efficiency ($CE_{max}$) across a range of $CIE_x$ or $CIE_y$ values, as discussed later. The fabricated TE devices followed the same device configurations as the simulated devices.

### *2.2. Green Hyperfluorescence™*

We designed and synthesized novel green TADF sensitizers and terminal FL emitters for high-performance HF OLEDs. Among various HF combinations, **G-HF1** and **G-HF2** were developed for practical use in AdobeRGB and BT.2020 chromaticity, respectively. Both combinations employed the same host and TADF materials, along with the respective FL dopants tailored for the AdobeRGB and BT.2020 color gamuts. To investigate their EL performance, we fabricated the BE devices for **G-HF1** and **G-HF2**. The device performance is summarized in Table 1.

Device **G-HF1** showed a green emission centered at 529 nm with an FWHM of 28 nm, as shown in Figure 2. It achieved an EQE of 25.2% and an $LT_{95}$ (95% of the initial luminance) of 1,500 h at 10 mA $cm^{-2}$. To further investigate the TE performance, we used Setfos 5.1 to perform a TE simulation for **G-HF1**, assuming a device configuration is similar to its BE device with a recombination zone near the EML/HBL interface. The $CE_{max}$ was estimated to be 199 cd $A^{-1}$ at $CIE_{x,y}$ coordinates of (0.210, 0.756), closely aligning with the definition of AdobeRGB green color coordinates of (0.210, 0.710).

For comparison, we benchmarked Device **G-HF1**'s performance against our 2023 green HF OLEDs developed for the same Adobe RGB chromaticity. The selected BE green HF device from 2023 showed the same emission maximum at 529 nm but with a slightly broader FWHM of 32 nm. It attained an EQE of 27.2% and an $LT_{95}$ of 477 h at 10 mA $cm^{-2}$. A TE device for this 2023 green HF OLED was also fabricated under a similar device configuration. The $CE_{max}$ achieved as high as 205 cd $A^{-1}$ at $CIE_{x,y}$ coordinates of (0.210, 0.754), nearly identical to its calculated result of 207 cd $A^{-1}$ at $CIE_x$ of 0.21. Compared to the 2023 green HF OLEDs, **G-HF1**, incorporating the new host, TADF, and dopant, significantly improved the $LT_{95}$ by more than 3 times without a drastic compromise in efficiency. This enhancement is primarily attributed to the improved structural stability of the new TADF in **G-HF1**. Additionally, the FWHM of the BE green HF devices was reduced from 32 to 28 nm, which contributes to better color purity and TE efficiency.

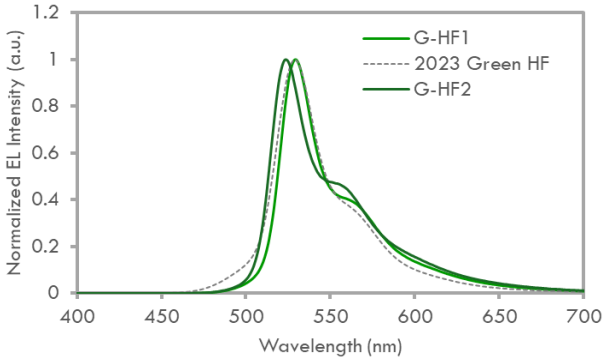


**Figure 2.** Normalized bottom-emission EL spectra of green Hyperfluorescence™ device **G-HF1**, 2023 green HF, and **G-HF2**.

In contrast, Device **G-HF2** showed a pure green emission centered at 523 nm with an FWHM of 32 nm in the BE device structure (Figure 2). Compared to Device **G-HF1**, the emission peak of **G-HF2** was blue-shifted by 6 nm, which is realized by substituting the terminal FL dopant in **G-HF1** to match the spectral requirements for BT.2020 applications. Device **G-HF2** demonstrated an EQE of 23.0% and an $LT_{95}$ of 970 h at 10 mA $cm^{-2}$. By employing the same host and TADF materials as Device **G-HF1**, Device **G-HF2** also achieved a long $LT_{95}$ without considerably compromising efficiency. Similarly, we used Setfos 5.1 to simulate the TE efficiency of **G-HF2**. Assuming the recombination zone was near the EML/HBL interface and a device configuration similar to its BE device, the $CE_{max}$ was estimated to be 160 cd $A^{-1}$ at $CIE_{x,y}$ coordinates of (0.170, 0.776), matching the definition of BT.2020 green color coordinates of (0.170, 0.797).

### *2.3. Red Hyperfluorescence™*

We also develop red TADF sensitizers to achieve high-performance red HF OLEDs for DCI-P3 and BT.2020 chromaticity applications. Combining the same red TADF

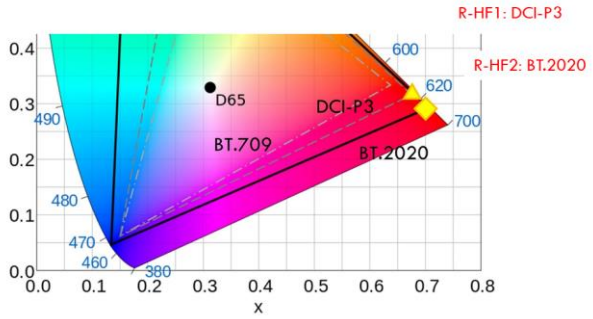


**Figure 3.** The $CIE_{x,y}$ coordinates of **R-HF1** and **R-HF2**.

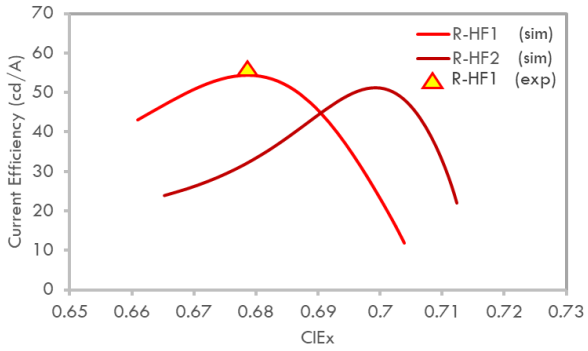


**Figure 4.** The simulated current efficiency against $CIE_x$ of the top-emission red Hyperfluorescence™ devices, **R-HF1** and **R-HF2,** as well as the experimental result of the TE device of **R-HF1**.

material with the respective red dopants, **RD1** and **RD2**, we developed **R-HF1** and **R-HF2** to match the color coordinates of DCI-P3 and BT.2020 definitions, respectively (Figure 3). To examine the device performance of **R-HF1** and **R-HF2,** both devices were fabricated in the BE structure. The device data are summarized in Table 1. Devices **R-HF1** and **R-HF2** displayed an EL maximum at 620 and 632 nm with an FWHM of 29 and 31 nm, respectively. Device **R-HF1** achieved an EQE of 16.9% and an $LT_{95}$ greater than 1,800 h. We also fabricated a TE device for **R-HF1** to investigate its device performance in DCI-P3 chromaticity. The $CE_{max}$ of the TE device was 57 cd $A^{-1}$ at $CIE_{x,y}$ coordinates of (0.680, 0.321), which is highly consistent with our simulation results, as shown in Figure 4. This result also demonstrates that **R-HF1** nicely translates the red definition of DCI-P3 with a $CIE_{x,y}$ coordinates of (0.680, 0.320).

In contrast, Device **R-HF2** exhibited an EQE of 14.9% and an $LT_{95}$ of 1,700 h. Simulations were conducted to estimate the TE performance of **R-HF2**. We assumed the recombination zone was near the EBL/EML interface, and the device configuration resembles its BE device. The expected CE as a function of $CIE_x$ is depicted in Figure 4. The $CE_{max}$ was estimated to be 51 cd $A^{-1}$ at $CIE_{x,y}$ coordinates of (0.700, 0.301), which aligns with the red definition of BT.2020, where the target color coordinates are (0.706, 0.292).

### *2.4. Blue Hyperfluorescence™*

Highly efficient and robust deep-blue OLED emitting technology has long been desired. Among emerging blue-emitting technologies, deep-blue HF OLEDs enabled by TADF sensitization are considered the ultimate solution due to their

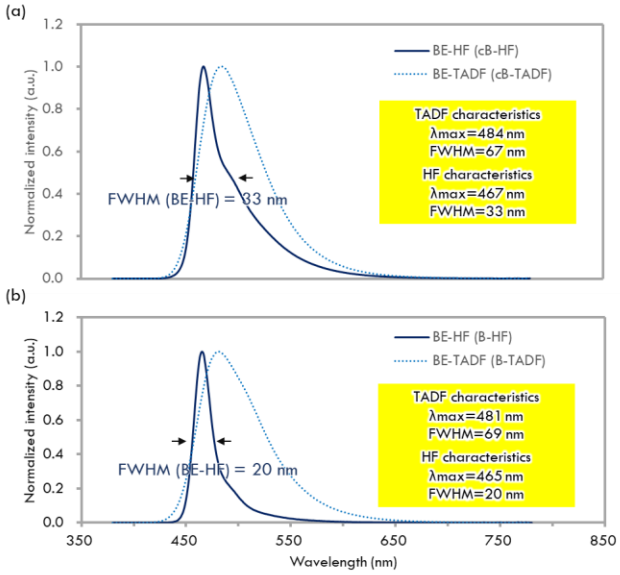


**Figure 5.** Normalized bottom-emission EL spectra of blue TADF and Hyperfluorescence™ devices. (a) cB-TADF vs. cB-HF, (b) B-TADF vs. B-HF. Inlets: the bottom-emission device characteristics of the respective device.

100% exciton harvesting ability and narrow-band emission. However, achieving a satisfactory lifetime is still highly desirable for practical use.

Recently, we developed a new sky-blue TADF material (**B-TADF**) that effectively sensitizes a deep-blue terminal FL emitter (**BD**). The combination of **B-TADF** and **BD** forms the new deep-blue HF, **B-HF**. We fabricated a BE device based on **B-HF** to investigate its device characteristics. The device data are summarized in Table 1. Device **B-HF** exhibited an emission centered at 465 nm with an FWHM of 20 nm, where an EQE of 23.9% was achieved. It is noteworthy that a deep-blue HF attained such a narrow BE emission bandwidth despite using a sky-blue TADF sensitizer, which is typically seen as a non-ideal HF combination due to ineffective FRET between the sensitizer and emitter. In light of the exceptional sharp emission and high efficiency of the BE deep-blue HF, we also fabricated a TE device for **B-HF** to examine its blue index performance. At a luminance of 1,000 nits, the TE device achieved a remarkable blue index of 417 cd/A/$CIE_y$ with $CIE_{x,y}$ coordinates of (0.133, 0.051), along with a narrow emission bandwidth with an FWHM of 14 nm.

To further explore the role of **B-TADF** in **B-HF**, we also fabricated BE devices for **B-TADF**. The performance of BE devices based on **B-TADF** and **B-HF** were compared with those of conventional sky-blue TADF (**cB-TADF**) and the corresponding conventional deep-blue HF (**cB-HF**), respectively. Both **B-HF** and **cB-HF** consist of **BD** at 0.3 wt% in the common host (BH), with **B-TADF** and **cB-TADF** at 30 wt%, respectively. Similarly, **B-TADF** and **cB-TADF** were doped at 30 wt% in BH in their respective BE TADF devices.

Figure 5 shows the EL spectra of **B-TADF**, **cB-TADF**, **B-HF**, and **cB-HF**. Device **B-TADF** and **cB-TADF** emitted at a similar sky-blue regime of 481 and 484 nm, respectively. Nonetheless, Device **B-HF** and **cB-HF** showed distinct FWHMs of 20 and 33 nm, respectively. We infer that the broader emission profile of Device **cB-HF** results from residual TADF emission due to

**Table 1.** Device performance of red, green, and blue Hyperfluoresence™

| At 10 mA/cm$^2$ | G-HF1 | G-HF2 | R-HF1 | R-HF2 | B-HF |
|---|---|---|---|---|---|
| $\lambda_{em}$ (nm) | 529 | 523 | 620 | 632 | 465 |
| FWHM (nm, BE) | 28 | 31 | 29 | 31 | 20 |
| EQE (%, BE) | 25.2 | 23.0 | 16.9 | 14.9 | 23.9 |
| $LT_{95}$ (h, BE) | 1500 | 970 | >1800 | 1700 | - |
| $CIE_{x,y}$ (TE) | (0.210, 0.756) | (0.170, 0.776) | (0.680, 0.321) | (0.700, 0.301) | (0.133, 0.051) |
| CE (cd/A, TE) | 199* | 160* | 57 | 51** | 417*** |

*Simulation results with a recombination zone setting near the HBL/EML interface. **Simulation results with a recombination zone setting near the EBL/EML interface. ***Blue index (cd/A/CIEy).

incomplete FRET between **cB-TADF** and **BD**. In contrast, **B-TADF**, emitting at a bluer regime by 3 nm with a slightly broader FWHM, enables a sufficient FRET to **BD**. A similar efficient sensitization behavior activating deep-blue HFs by greenish TADFs has been previously reported by Stavrou *et al*. [5]. The key to enabling this mechanism is that the FRET rate of TADF sensitizers needs to prevail over other deactivation processes, including radiative and nonradiative relaxations, even when the spectral overlap between TADF sensitizers and terminal FL emitters is minimal. Furthermore, a rapid rISC rate of the sensitizers is still essential to suppress triplet energy loss via other unwanted competitive deactivations. We observed similar exciton dynamics in **B-TADF**, which we believe contribute to the different FWHM outcomes between **B-HF** and **cB-HF**. To unwind the mechanism behind it, we are conducting more relevant photophysical studies and exploring more promising TADF candidates from our materials library.

This blue study demonstrates that a highly efficient deep-blue HF OLED with a narrow emission bandwidth can be realized by incorporating a lower energy TADF sensitizer, while still achieving complete FRET, which used to be regarded as a non-ideal HF combination. The approach of utilizing low-energy sensitizers to activate high-energy emitters substantially benefits device longevity. The pursuit of deep-blue sensitizers is no longer necessary, while the requirement on high $T_1$ hosts can be significantly mitigated.

Although the lifetime of the current deep-blue HF has not yet met the industry's requirement, we believe this work provides a practical approach to allow deep-blue HF OLEDs to have a satisfactory lifetime without compromising the color and efficiency performance, which can expedite the commercialization of deep-blue HF OLEDs. We are aggressively engaging in the stability improvement of both TADF sensitizers and FL emitters by exploiting our proprietary AI materials informatics platform, Kyumatic™, to address the remaining challenges. Kyumatic™, which integrates mass molecular generation, quantum computation, and high-accuracy physical property prediction, streamlines the lengthy materials exploration process. By leveraging its powerful machine-learning capability and high-throughput virtual screening, we believe that the combination of low-energy sensitization and Kyumatic™ will be groundbreaking in overcoming the last bottleneck in deep-blue HF development.

## 3. Summary

In this work, we demonstrated highly efficient green, red, and blue HF OLEDs with remarkable color purity across various color spaces. **G-HF1** and **G-HF2** were developed to meet the green standards of AdobeRGB and BT.2020 chromaticity, respectively. By incorporating the structurally stable novel TADF sensitizer, both green HF achieved a significant $LT_{95}$ breakthrough of 1,500 and 970 h at 10 mA cm$^{-2}$, respectively. In addition, **G-HF1** emitting at 529 nm reached a high EQE of 25.2% with a very narrow FWHM of 28 nm in the BE device. This contributes to a high estimated TE efficiency of 199 cd/A at $CIE_{x,y}$ coordinates of (0.210, 0.756). This achievement has met the requirements of our customers, and we are currently working closely with them to finalize the last short step toward commercialization.

Meanwhile, the development of red HF OLEDs is also progressing toward commercialization. The red devices of **R-HF1** and **R-HF2**, designed for DCI-P3 and BT.2020 chromaticity, exhibited narrow FWHMs of 29 and 31 nm and long $LT_{95}$ of over 1,800 h and 1,700 h, respectively. The TE efficiency for **R-HF1** and **R-HF2** was estimated to be 57 cd/A at $CIE_{x,y}$ of (0.680, 0.321) and 51 cd/A at (0.700, 0.301) at 10 mA cm$^{-2}$. The device optimization to boost the red performance is ongoing.

Notably, an unprecedented high blue index of 417 cd/A/$CIE_y$ at $CIE_y$ of 0.05 has been realized by a sky-blue TADF material without compromising color purity. In this report, we demonstrated that high-energy TADFs are no longer a necessary criterion for achieving outperformed deep-blue HF OLEDs. This new approach opens a grand window to expedite the commercialization process for deep-blue HF OLEDs. Furthermore, leveraging our proprietary AI materials informatics system, Kyumatic™, we anticipate that material exploration can be accelerated hundreds of folds.

## 4. Acknowledgements

This work was partly supported by Japan Science and Technology Agency (JST) (project no. JPMJTT22J1) and the New Energy and Industrial Technology Development Organization (NEDO) (project no. JPNP 21005).

## 5. References

1. Nakanotani H. et al., High-efficiency organic light-emitting diodes with fluorescent emitters, Nat. Commun. 5, 4016-4022 (2014).
2. Hatakeyama T. et al., Ultrapure blue thermally activated delayed fluorescence molecules: efficient HOMO-LUMO separation by the multiple resonance effect, Adv. Mater. 28, 2777-2781 (2016).
3. Tasaki S. et al., Realization of ultra-high-efficient fluorescence blue OLED, J Soc Inf Display 30, 441-451 (2022).
4. Recommendation ITU-R BT.2020, Parameter values for ultra-high definition television systems for production and international programme exchange, 2012.
5. Stavrou K. et al., Key requirements of ultraefficient sensitization in Hyperfluorescence organic light-emitting diodes, Nat. Photon. 18, 554-561 (2024).